Economic Geology
Vol. 91, 1996, pp. 549–562

Galena Lead Isotopes, Buttle Lake Mining Camp, Vancouver Island, British Columbia, Canada

COLIN I. GODWIN, MICHELLE ROBINSON,*

Mineral Deposits Research Unit, Department of Geological Sciences, University of British Columbia, Vancouver, British Columbia, Canada V6T 1Z4

AND STEPHEN J. JURAS

Westmin Resources Limited, Myra Falls Operations, P.O. Box 8000, Campbell River, British Columbia, Canada V9W 5E2

Abstract

Volcanogenic massive sulfide deposits within the Buttle Lake mining camp are associated with andesitic and felsic rocks of the Price and Myra formations in the Paleozoic Sicker Group. The Sicker Group forms the oldest known unit within the Wrangellia terrane.

Lead isotope data for galena from the Buttle Lake mining camp indicate that lead evolved in an orogen or island-arc environment. There is a pronounced linear trend in the lead isotope data that can be explained as a mixing line. Positions of data along this trend do not relate to age differences among the ore lenses or to variable selective leaching of lead isotope components from significantly older footwall source rocks. However, the line appears to represent one or a combination of (1) variable mixing of lead from felsic and andesitic rocks (or related magmatic fluids), each with distinctly different proportions of upper crustal and mantle lead isotopes, or (2) mixing of lead isotopes from relatively radiogenic oceanic sediment with relatively primitive lead isotopes from the volcanic rocks (or related magmatic fluids).

More specifically, the less radiogenic end member appears to be spatially related to rhyolitic host rocks. The rhyolitic rocks may have contributed a magmatic component or represent leached source rocks of the same age as the mineralization. The more radiogenic deposits generally occur immediately above major discharge stockworks in andesite. The andesites may have a distinctive, relatively radiogenic magmatic source, or contain interbeds of more radiogenic oceanic sediment.

Markedly radiogenic lead characterizes most deposits within the H-W horizon, defined in part, by the H-W Main and Battle Main lenses. These lenses, immediately above the Price formation contact, are among the largest; consequently, relatively radiogenic lead isotope compositions may identify the most favorable exploration targets.

Introduction

BUTTLE LAKE mining camp (NTS: 092F12E; 49°34′ N, 125°36′ W), near central Vancouver Island in Strathcona Park at the south end of Buttle Lake, is 90 km southwest of Campbell River, southwestern British Columbia (Fig. 1). The camp is a major volcanogenic massive sulfide district with deposits in the Myra formation of the Paleozoic Sicker Group (Table 1). Past production has come from several mines: Lynx (open pit and underground), Myra (open pit and underground), and H-W (underground). The Price deposit, discovered early in the history of the camp, has received sporadic work but has not been mined. Current production is from the H-W mine. Between 1966 and 1992, 13.8 million metric tons (Mt) of ore grading 1.9 percent copper, 5.6 percent zinc, 0.6 percent lead, 2.2 g/t gold, and 64.0 g/t silver were mined from the camp (Westmin Annual Report, 1992). Of this, 7.5 Mt were from the H-W, 5.3 Mt from the Lynx, and 1.0 Mt from the Myra mine (Pearson, 1993). Geologic reserves at the end of 1992 total about 12.5 Mt. These include, for recently discovered but unmined deposits, 2.0 Mt for the Battle and 0.6 Mt for the Gap. Exploration within the camp also has defined several new prospective zones including: Trumpeter, Ridge, and the Main zone extension (Fig. 2).

Previous work on the Buttle Lake deposits by Andrew (1987) and Andrew and Godwin (1989) established that Sicker Group lead isotope ratios of galena and for whole rocks (adjusted to deposit age) have higher $^{207}Pb/^{204}Pb$ ratios than midocean ridge basalts and resemble other island arcs, and that galena from the Myra deposit has $^{206}Pb/^{204}Pb$ and $^{208}Pb/^{206}Pb$ isotope ratios which are statistically different from the H-W deposit (Figs. 1 and 2); thus, they concluded that galena lead isotope data might be useful in defining ore genesis, and in distinguishing and correlating ore lenses within the Buttle Lake camp.

This paper presents the results of 103 lead isotope analyses of 53 galena samples from 19 sulfide lenses or zones in the H-W and Lynx-Myra-Price horizons (Table 2). Sample locations are given in Figures 2 and 3. It is demonstrated that lead isotope signatures are correlated with the compositions of footwall rocks, and that galena lead isotopes are indeed useful for distinguishing and correlating ore lenses. Finally, several isotopic models are examined to explain the linear variations in isotopic compositions among the ore lenses. The slopes of the galena lead isotope data for the ore lenses are consistent with lead derived by mixing of mantle and upper crust lead isotopes. Two explantions of how this might have been accomplished are discussed.

Regional Geology

Massive sulfide deposits of the Buttle Lake mining camp occur within the Myra formation of the Paleozoic Sicker

* Present address: Robinson Resources, Inc, 309 10675 138A Street, Surrey, British Columbia, Canada V3T 4L3.

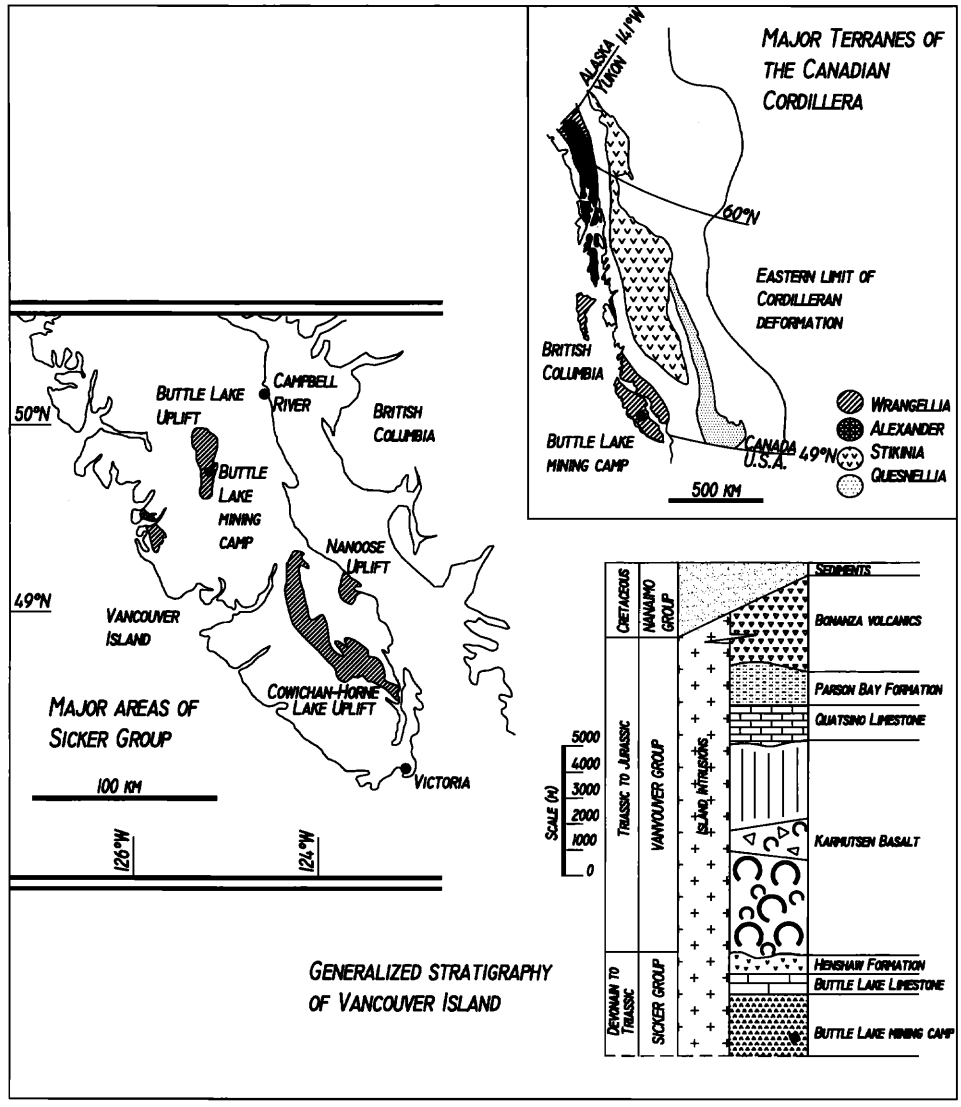

FIG. 1. Location map showing the Buttle Lake mining camp within the Paleozoic Sicker Group of the Wrangellia terrane (Jones et al., 1977). The stratigraphic column of Vancouver Island is simplified from Muller et al. (1974) and Juras (1987).

Group. The Sicker Group is the oldest stratigraphic unit recognized on Vancouver Island and represents the base of Wrangellia, an allochthonous terrane that underlies most of the island (Jones et al., 1977). The Sicker Group in exposed by three major fault-bounded uplifts: Buttle Lake, Cowichan-Horne Lake, and Nanoose (Fig. 1). The Buttle Lake camp occurs in the Buttle Lake uplift.

A revised stratigraphy for the Buttle Lake uplift is found in Table 1. This table of formations, established by Juras (1987), incorporates earlier work by Yole (1969), Jeffery (1970), and Muller (1980). In order of decreasing age the formations recognized (all informal) are Price, Myra, Thelwood, Flower Ridge, Buttle Lake, and Henshaw.

Mine Geology: The Price and Myra Formations

Price formation andesite underlies the ore-bearing Myra formation. The Myra formation is a complex sequence of mafic to rhyolitic volcaniclastic rocks and lesser flow units that fill a northwest-trending basin. Only the details of the Price and Myra formations that are relevant to this paper are discussed below.

Price formation

The Price formation (Fig. 3), as observed in the uppermost 300 m explored (its base has not been identified), is a sequence of massive to pillowed basaltic andesite flows, volcanic breccias, interflow clastic sediments, and turbidites. Basaltic andesite flows are of two types (Juras, 1987): pyroxene-feldspar porphyritic, and feldspar-porphyritic. Contacts to individual flow units may be massive, devitrified glass, or quench brecciated. Pillow breccia is also common. Interflow sediments are volumetrically insignificant (about 5% of the explored section) and consist of gray to green graywacke and

TABLE 1. Table of Formations within the Paleozoic Sicker Group in the Buttle Lake Uplift, Central Vancouver Island, Southwestern British Columbia (modified from Juras, 1987)

Age	Formation	Thickness (m)	Lithology
Early Permian (?) to Early Triassic	Henshaw	5–100	Conglomerate, epiclastic deposits, and pumiceous tuff
Early Permian to Pennsylvanian[1]	Buttle Lake	300	Crinoidal limestone and minor chert
Mississippian to Early Permian[2]	Flower Ridge	650+	Moderately to strongly amygdaloidal mafic lapilli tuff (scoria clast), tuff breccia, minor tuffs and flows, and syndepositional(?) sills[2]
Early Mississippian (?)	Thelwood	250–500	Subaqueous pyroclastic deposits, siliceous tuffaceous sediments, and mafic sills
Late Devonian[3]	Myra	300–450	Intermediate to felsic volcanics, volcaniclastics, minor sediments, and massive sulfide mineralization
Late Devonian or older	Price	300+	Feldspar-pyroxene porphyritic basaltic andesite flows, flow breccias, and minor sediments

[1] Pennsylvanian to Early Permian based on brachiopods (Fyles, 1955), fusulinids (Sada and Danner, 1974), foraminifera (Muller et al., 1974), and conodonts (Brandon et al., 1986)

[2] 276 ± 8 Ma, K-Ar hornblende: Early Permian (unpublished data: C. Godwin, J. Harakal, and D. Runkle, Geochronology Laboratory, University of British Columbia)

[3] 370 ± 6 Ma, U-Pb zircon (Juras, 1987)

shale. They commonly are moderately well sorted and fine upward; some are turbidites.

Myra formation

Ten lithostratigraphic units were recognized in the Myra formation by Juras (fig. 3; 1987). The six lower ones in Figure 3 host all known ore occurrences. From the base upward these six are the following:

1. H-W horizon[1] (Fig. 3), mainly of felsic flows and volcaniclastics (Walker, 1985), is 15 to 200 m thick and occurs

[1] The use of the term "horizon" to describe the ore-bearing or ore equivalent lithologic units comes from Sangster (1972) and is embedded in the mine terminology and literature on the Buttle Lake deposits. For this reason the terms "H-W horizon" and "Lynx-Myra-Price horizon" are retained in this paper, although the word "horizon" usually refers to a distinctive very thin bed (Bates and Jackson, 1987).

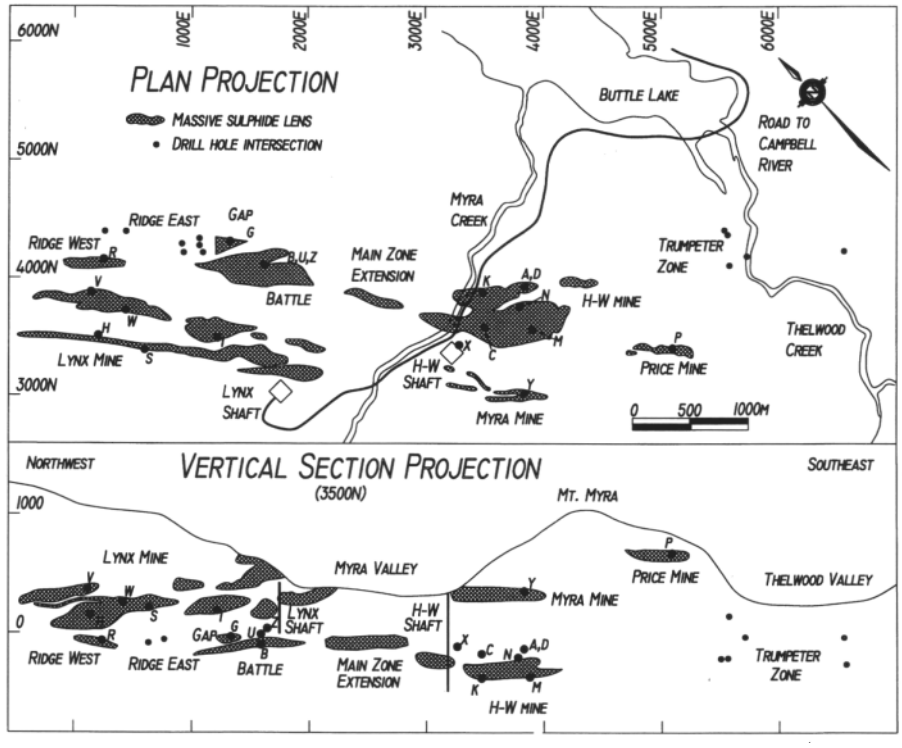

FIG. 2. Buttle Lake mining camp, central Vancouver Island, southwestern British Columbia (inset), showing the surface and vertical projections of the ore lenses for which analyses are presented in Table 4 (Westmin Resources Limited Annual Report, 1992). Note that mine coordinates are based on a northwest-trending grid. The ore lenses are identified by symbols that are defined in Tables 2, 3, and 5.

TABLE 2. Galena Lead Isotpe Data[1] for Orebodies in the Buttle Lake Mining Camp, Central Vancouver Island, Southwestern British Columbia

Sample no.	No. of runs	Lens or zone	Horizon[2]	Symbol (Figs. 2 and 3)	$^{206}Pb/^{204}Pb$	$^{207}Pb/^{204}Pb$	$^{208}Pb/^{204}Pb$	$^{207}Pb/^{206}Pb \times 100$	$^{208}Pb/^{206}Pb \times 10$
30735-018	2	Ore clast breccia	Ore-X	X	18.448	15.564	38.087	84.371	20.647
30316-001	2	Gap	H-W	G	18.483	15.567	38.100	84.222	20.614
30316-002	2	Gap	H-W	G	18.485	15.573	38.121	84.252	20.624
30316-003	1	Gap	H-W	G	18.495	15.577	38.145	84.230	20.627
30316-004	1	Gap	H-W	G	18.479	15.577	38.127	84.295	20.633
31145-016	1	Hanging wall	H-W	Z	18.490	15.579	38.145	84.252	20.630
30735-009	1	H-W North Bornite	H-W	N	18.508	15.570	38.126	84.123	20.600
30735-206	2	H-W North Bornite	H-W	N	18.476	15.567	38.100	84.251	20.620
30735-207	5	H-W North Bornite	H-W	N	18.504	15.574	38.116	84.160	20.611
30735-219	2	H-W North Bornite	H-W	N	18.493	15.575	38.129	84.218	20.617
30735-220	2	H-W North Bornite	H-W	N	18.480	15.560	38.085	84.199	20.608
31145-002	1	Battle Upper	H-W	U	18.491	15.570	38.125	84.205	20.618
31145-003	1	Battle Upper	H-W	U	18.515	15.572	38.144	84.107	20.602
31145-006	3	Battle Upper	H-W	U	18.501	15.581	38.153	84.216	20.622
31145-010	1	Battle Upper	H-W	U	18.491	15.567	38.111	84.186	20.610
31145-011	1	Battle Upper	H-W	U	18.513	15.580	38.161	84.160	20.614
31145-012	1	Battle Upper	H-W	U	18.509	15.587	38.171	84.212	20.623
31145-014	1	Battle Upper	H-W	U	18.489	15.575	38.134	84.241	20.626
31145-015	1	Battle Upper	H-W	U	18.498	15.575	38.180	84.198	20.613
31145-013	1	Battle Upper	H-W	U	18.504	15.580	38.153	84.199	20.619
30735-004	1	H-W Upper (A)	H-W	A	18.511	15.576	38.146	84.145	20.608
31145-018	1	Battle Main	H-W	B	18.510	15.575	38.145	84.144	20.608
31145-017	1	Battle Main	H-W	B	18.506	15.570	38.130	84.134	20.604
31145-019	1	Battle Main	H-W	B	18.499	15.563	38.104	84.129	20.598
31145-003	1	Battle Main	H-W	B	18.515	15.572	38.144	84.107	20.602
30443-216	2	Lynx (H)	Ore-X	H	18.516	15.579	38.164	84.134	20.611
30443-217	2	Lynx (I)	Ore-X	I	18.501	15.574	38.142	84.183	20.616
30703-001	1	Myra	L-M-P	Y	18.493	15.565	38.104	84.169	20.605
30703-002	1	Myra	L-M-P	Y	18.489	15.568	38.113	84.201	20.614
30703-202	3	Myra	L-M-P	Y	18.486	15.549	38.067	84.120	20.594
30703-203	3	Myra	L-M-P	Y	18.492	15.559	38.091	84.139	20.598
30703-204	2	Myra	L-M-P	Y	18.499	15.568	38.118	84.155	20.605
30703-201	1	Myra	L-M-P	Y	18.516	15.571	38.135	84.099	20.596
31145-005	1	Battle Main	H-W	B	18.575	15.578	38.200	83.868	20.566
31145-007	1	Battle Main	H-W	B	18.530	15.574	38.151	84.048	20.589
31145-008	1	Battle Main	H-W	B	18.541	15.580	38.175	84.033	20.590
31145-001	2	Battle Main	H-W	B	18.525	15.567	38.135	84.030	20.586
31145-009	1	Battle Main	H-W	B	18.586	15.590	38.240	83.884	20.575
30735-008	3	H-W:North (K)	H-W	K	18.566	15.574	38.178	83.888	20.565
30735-015	1	H-W Upper (C)	H-W	C	18.537	15.575	38.157	84.020	20.584
30735-217	3	H-W Upper (D)	H-W	D	18.533	15.572	38.147	84.027	20.584
30735-005	2	H-W Main	H-W	M	18.562	15.589	38.215	83.984	20.587
30735-202	2	H-W Main	H-W	M	18.553	15.577	38.171	83.960	20.574
30735-224	3	H-W Main	H-W	M	18.557	15.567	38.152	83.888	20.559
30735-007	2	Ridge West	H-W	R	18.554	15.582	38.195	83.983	20.586
30443-008	2	Lynx S	L-M-P	S	18.573	15.582	38.203	83.895	20.568
30443-208	3	Lynx S	L-M-P	S	18.540	15.564	38.135	83.950	20.569
30443-209	3	Lynx S	L-M-P	S	18.556	15.568	38.147	83.889	20.558
30443-006	2	Lynx West G (W)	L-M-P	W	18.552	15.577	38.172	83.964	20.576
30443-201	2	Lynx West G (V)	L-M-P	V	18.548	15.574	38.158	83.965	20.576
30443-203	2	Lynx West G (V)	L-M-P	V	18.549	15.575	38.162	83.965	20.574
30443-204	12	Lynx West G (W)	L-M-P	W	18.563	15.572	38.170	83.887	20.562
30360-001	3	Price	L-M-P	P	18.534	15.568	38.140	84.000	20.580

[1] All analyses were done by A. Pickering, Geochronometry Laboratory, Department of Geological Sciences, University of British Columbia
[2] Mine nomenclature uses "horizon": H-W = H-W horizon; L-M-P = Lynx-Myra-Price horizon; Ore-X = ore clast breccia

throughout the mine area. There are seven members within the H-W horizon (Juras, 1987; Juras and Pearson, 1990; Robinson et al., 1994): massive sulfide lenses, argillite-chert, H-W mafic sills, pumiceous lapilli tuff, rhyolitic tuff, upper zone massive sulfide lenses, and a felsic flow dome complex. Major massive sulfide lenses (Figs. 2 and 3), including the H-W Main lens (M), H-W North lenses (N and K), and the Battle Main zone (B), occur at the contact with the Price formation and form the base of the H-W horizon. Upper zone massive sulfide lenses occur both within and at the top of the rhyolitic tuff. These include the H-W Upper zone (A, C, and D) lenses, the Ridge West (R) zone lens, and the Battle Upper (U) lenses.

2. Hanging-wall andesite (Fig. 3) consists mostly of basaltic

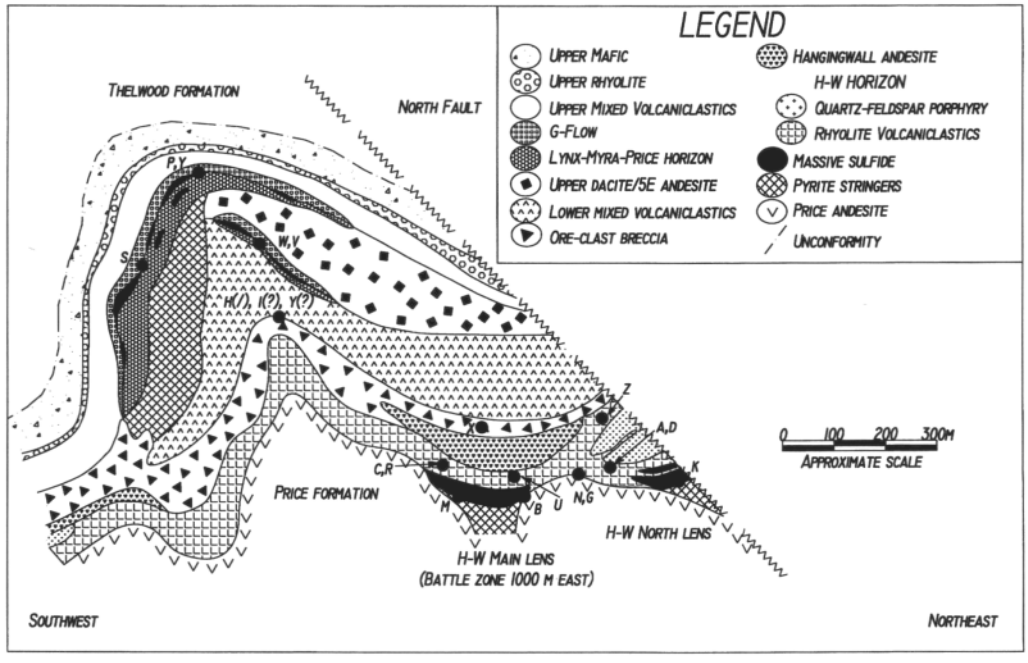

FIG. 3. Diagrammatic cross section of the Buttle Lake camp showing location of ore lenses in the Myra formation projected onto a stratigraphic section at about 2,000 m east (Fig. 2; compiled from Juras, 1987, and Pearson, 1993). Units are not all continuous out of the section. The lower mixed volcaniclastics unit in the anticlinal core region is supplanted by 5E andesite at the west end of the camp (samples W and V). Also the stringer zone below the south limb of the Lynx-Myra-Price horizon lies within 5E andesite. Ore lenses are identified by symbols defined in Tables 2, 3, and 5. The lenses are located in projected plan and cross section in Figure 2.

andesite flows and shallow-level sills that locally intrude the H-W horizon (Barrett et al., 1994) and flow breccias. The unit is up to 100 m thick; individual flow members can be over 20 m thick. The hanging-wall andesite is thickest over the H-W Main lens, probably because that lens was deposited in a topographic low (Pearson, 1993).

3. Ore-clast breccia (Fig. 3) is characterized by massive sulfide clasts and olistoliths of pyrite-mineralized rhyolite up to 50 m long by 15 m wide (Juras, 1987; Juras and Pearson, 1990). The unit is up to 90 m thick and consists of a series of submarine debris flows and lesser pyroclastic deposits. Clast types are variable. In decreasing order of abundance they are feldspar-porphyritic andesite, amygdaloidal mafic, dacite, quartz feldspar porphyritic rhyolite, massive sulfide, fine rhyolite tuff, chert, and argillite.

4. Lower mixed volcaniclastics (Fig. 3) are dominated by andesite that contains lesser dacite fragments. The unit also includes rare thin flows of andesite. The unit, as thick as 90 m, contains bedded clastic sequences and coarse clastic deposits (Juras, 1987).

5. Upper dacite-5E andesite (Fig. 3) occurs at the southeast and northwest ends of the mine property, respectively. The upper dacite, as much as 60 m thick, contains resedimented hyaloclastite, pillow breccia, and subaqueous pyroclastic deposits, and intermediate flows. The 5E andesite sequence of massive to pillowed basaltic andesite flows and flow breccias is as thick as 250 m. The upper dacite and the 5E andesite represent two contemporaneous, but distinct, eruptive events (Juras, 1987).

6. The Lynx-Myra-Price horizon (Fig. 3), as much as 60 m thick, comprises (Juras, 1987) massive to bedded, fine to coarse tuff; quartz-feldspar crystal and pumiceous rhyolite lapilli tuff; and lesser chert. Massive sulfides lenses occur at two levels within the Lynx-Myra-Price horizon. Some lenses are located at the base of the horizon where they are underlain by schistose sericite-quartz-pyrite feeder zones within the 5E andesite. Other lenses occur at the upper contact of this horizon with the G flow (Fig. 3). These lenses lie on top of rhyolitic tuffs without distinctive underlying feeder zones. They are composed of banded sphalerite, barite, pyrite, chalcopyrite, galena, and tennantite.

Galena Lead Isotope Analyses

A small (<0.1 g) cleavage cube of galena was handpicked from each sample and analyzed by Ann Pickering at the Geochronology Laboratory, Department of Geological Sciences, University of British Columbia. The analyses were done by the silica gel-phosphoric acid method using a single filament on a Vacuum Generators Ltd. Isomass 54R solid source mass spectrometer; results were normalized to the NBS 1 standard (for details see Godwin et al., 1988). Lead isotope data for galena from the Buttle Lake camp are presented in Tables 2 and 3, and Figures 4 and 5.

Sources of error in mass spectroscopic measurement of lead isotopes include overall analytical error, ^{204}Pb error, and fractionation error. Based on repeated analysis of the NBS 1 standard, analytical errors at 2σ are on the order of 0.1 percent for $^{206}Pb/^{204}Pb$, $^{207}Pb/^{204}Pb$, and $^{208}Pb/^{204}Pb$, but 0.05 percent for ($^{207}Pb/^{206}Pb \times 100$) and ($^{208}Pb/^{206}Pb \times 10$). The ^{204}Pb error and fractionation error depend to a large extent

TABLE 3. Average Galena Lead Isotpe Ratios[1] for Lenses within the Buttle Lake Mining Camp, Southwestern British Columbia

Name	No. of runs	Lens	Horizon[2]	Symbol (Figs. 2 and 3)	Rank order (based on Fig. 5d)	$^{206}Pb/^{204}Pb$	$^{207}Pb/^{204}Pb$	$^{208}Pb/^{204}Pb$	$^{207}Pb/^{206}Pb \times 100$	$^{208}Pb/^{206}Pb \times 10$
Ore	1	Ore clast breccia[3]	Ore-X	X	1	18.448	15.564	38.087	84.371	20.647
Hanging wall	1	Hanging wall zone	H-W	Z	2	18.490	15.579	38.145	84.252	20.630
Gap	4	Gap	H-W	G	3	18.486	15.575	38.128	84.250	20.626
Battle	9	Battle Upper	H-W	U	4	18.501	15.576	38.148	84.192	20.616
Lynx	1	Lynx (1)	Ore-X	I	5	18.501	15.574	38.142	84.183	20.616
H-W	5	H-W North Bornite	H-W	N	6	18.492	15.569	38.111	84.190	20.611
H-W	1	H-W Upper (A)	H-W	A	7	18.511	15.576	38.146	84.145	20.608
Lynx	1	Lynx (H)	Ore-X	H	8	18.516	15.579	38.164	84.134	20.611
Myra	6	Myra	L-M-P	Y	9	18.496	15.563	38.105	84.147	20.602
Battle	4	Battle Main	H-W	B	10	18.508	15.570	38.131	84.129	20.603
H-W	1	H-W Upper (D)	H-W	D	11	18.533	15.572	38.147	84.027	20.584
H-W	1	H-W Upper (C)	H-W	C	12	18.537	15.575	38.157	84.020	20.584
Price	1	Price	L-M-P	P	13	18.534	15.568	38.140	84.000	20.580
Ridge	1	Ridge West	H-W (?)	R	14	18.554	15.582	38.195	83.983	20.586
Battle	5	Battle Main	H-W	B	15	18.551	15.578	38.180	83.973	20.581
Lynx	2	Lynx West G (V)	L-M-P	V	16	18.549	15.574	38.160	83.965	20.574
H-W	3	H-W Main	H-W	M	17	18.557	15.578	38.179	83.944	20.573
Lynx	2	Lynx West G (W)	L-M-P	W	18	18.557	15.574	38.171	83.926	20.569
Lynx	3	Lynx S	L-M-P	S	19	18.556	15.571	38.162	83.911	20.565
H-W	1	H-W North (K)	H-W	K	20	18.566	15.574	38.178	83.888	20.565
Mean $\pm 2\sigma$	20	Ore lenses[3]				18.524 $\pm$ 0.064	15.573 $\pm$ 0.010	38.149 $\pm$ 0.054	84.073 $\pm$ 0.268	20.595 $\pm$ 0.046

[1] All analyses were done by A. Pickering, Geochronology Laboratory, Department of Geological Sciences, University of British Columbia
[2] Mine nomenclature uses "horizon": H-W = H-W horizon; L-M-P = Lynx-Myra-Price horizon; Ore-X = Ore clast breccia
[3] One estimate of Late Devonian orogen lead isotope values for the Wrangellia terrane, and more specifically, the Myra formation of the Sicker Group (see text)

on consistency of loading technique and run temperature and can sometimes be detected from trends in the analyses. Thus, slopes related to these errors are shown on the data plots (Fig. 5). Data are elongated parallel to these errors in Figure 5a and b but are not so affected in Figure 5c and d, the ($^{208}Pb/^{206}Pb \times 10$) versus ($^{207}Pb/^{206}Pb \times 100$) plots, where ^{204}Pb error is not present. Consequently, the trends parallel to the errors in Figure 5a and b are considered to reflect analytical error mainly and are not thought to be mixing trends. In addition, because of lesser analytical error on ($^{208}Pb/^{206}Pb \times 10$) versus ($^{207}Pb/^{206}Pb \times 100$) plots, this type of plot is emphasized in the analysis below.

Characteristics of Galena Lead Isotope Data from Buttle Lake Camp

Characterization as orogen lead

Lead isotope evolution, based on computer simulation of orogensis, was approximated for four major world-scale reservoirs by Zartman and Doe (1981; cf. Doe and Zartman, 1979): mantle, lower crust, upper crust, and orogen. Orogen lead isotope compositions, formed by mixing of lead from the four reservoirs by the subduction process, is characteristic of lead isotope compositions found in island arcs. Estimates of lead isotope values for the upper crust and mantle lead evolution curves used in Figure 4a to c are tabulated in Godwin et al. (1988).

Data from Table 2 plot between the upper crustal and mantle curves in Figure 4a to c: $^{207}Pb/^{204}Pb$ versus $^{206}Pb/^{204}Pb$ plot, $^{208}Pb/^{204}Pb$ versus $^{206}Pb/^{204}Pb$ plot, and ($^{208}Pb/^{206}Pb \times 10$) versus ($^{207}Pb/^{206}Pb \times 100$) plot, respectively. The lead apparently is orogenic in character because in all three plots it can be described as a mixture of upper crustal and mantle leads. In addition, Andrew (1987) and Andrew and Godwin (1989) showed that lead isotope ratios of galena and initial ratios of whole-rock samples of the Myra formation within the Sicker Group plot in the lead isotope field of present-day island arcs adjusted to the Late Devonian.

The mean for the galena lead isotope ratios of the ore lenses sampled should be a good approximation of orogenic Late Devonian lead isotope ratios in the Wrangellia terrane. The values and variation at two standard deviations for this are (Table 3) $^{206}Pb/^{204}Pb = 18.524 \pm 0.064$, $^{207}Pb/^{204}Pb = 15.573 \pm 0.010$, $^{208}Pb/^{204}Pb = 38.149 \pm 0.054$, ($^{207}Pb/^{206}Pb \times 100$) $= 84.073 \pm 0.268$, and ($^{208}Pb/^{206}Pb \times 10$) $= 20.595 \pm 0.046$. However, if the radiogenic end of the data array is caused by mixing with lead leached from interbedded oceanic or crustal sediments (see "Discussion," below), the values for the ore clast breccia should be closer to the overall orogen value. These less radiogenic values are (Table 3): $^{206}Pb/^{204}Pb = 18.448$, $^{207}Pb/^{204}Pb = 15.564$, $^{208}Pb/^{204}Pb = 38.087$, ($^{207}Pb/^{206}Pb \times 100$) $= 84.371$, and ($^{208}Pb/^{206}Pb \times 10$] $= 20.647$.

The world-scale model for lead evolution is only an approximation; it does not define the Late Devonian age of the deposits. In Figure 4a to c the lead analyses plot near mixing lines between the upper crust and mantle curves for the Triassic (Fig. 4c) and Cretaceous (Fig. 4a). On these plots, the orebodies appear superficially to be much younger than their true age. Furthermore, the estimated orogen curve of Zartman and Doe (1981) would predict an even younger age.

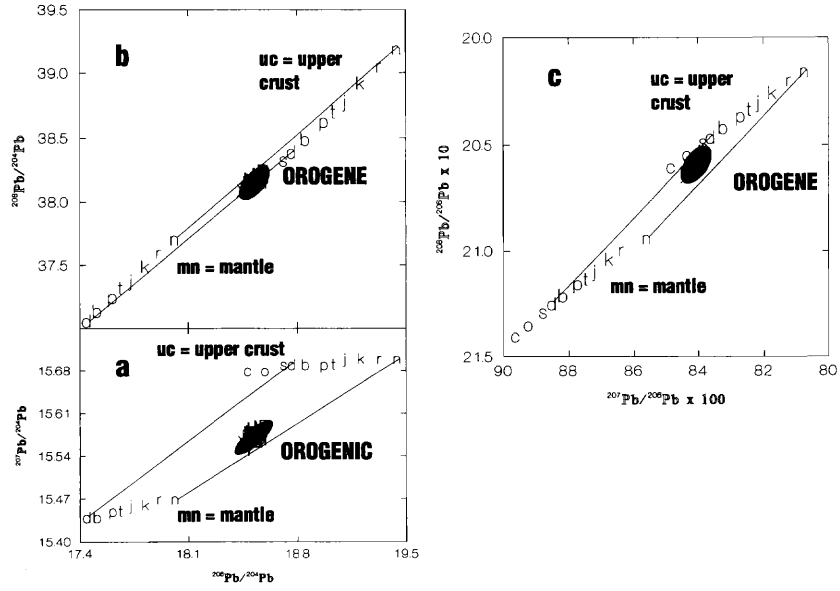

FIG. 4. Large-scale galena lead isotope plots for the Buttle Lake mining camp, southwestern British Columbia. Data are from Table 2. (a). $^{207}Pb/^{204}Pb$ versus $^{206}Pb/^{204}Pb$ plot. (b). $^{208}Pb/^{204}Pb$ versus $^{206}Pb/^{204}Pb$ plot. (c). ($^{208}Pb/^{206}Pb \times 10$) versus ($^{207}Pb/^{206}Pb \times 100$) plot. Upper crust and mantle plumbotectonic curves are after Zartman and Doe (1981; Godwin et al., 1988). Data from the Buttle Lake deposits, typical of island-arc or orogen lead, cluster between the two curves. The age cannot be estimated from the plumbotectonic curves. Mixing lines are shown for the base of the Devonian (d) and for the present day (n). The model curves have the base of each age period plotted as: s = Silurian, b = Carboniferous, c = Cambrian, d = Devonian, j = Jurassic, k = Cretaceous, n = now, o = Ordovician, p = Permian, r = Tertiary, and t = Triassic.

Characterization as clusters along a line

Galena lead isotope data (Table 2) for the Buttle Lake ore lenses plot in two clusters and an outside point X in Figure 5a to d. Elongation of the clusters in the direction of fractionation and ^{204}Pb error make the two clusters look particularly distinctive in Figure 5a and b. However, in Figure 5c and d, where ^{204}Pb error is absent, the error trends are not as apparent, and the two clusters and the outside point X look colinear. Differences in analyses of specific lenses within the clusters (e.g., U = Battle Upper, G = Gap, and S = Lynx S) are greater than the spaces between the clustered data and outside point X. In addition, several lenses plot in both clusters (B = Battle Main; A, C, and D = H-W Upper; and N and K = H-W North). This reinforces the interpretation of the data as linear arrays. However, it was the distinctive difference between Myra (Y) and H-W Main (B) that was noted by Andrew and Godwin (1989).

We conclude, therefore, that the galena lead isotope data from Buttle Lake ore lenses can be characterized as two clusters and an outside point X along a trend that can be approximated by a line. Table 4 defines the slopes of the lines (dt) through the ore lens isotopic data of Table 2 and Figure 5a to c, respectively, as indeterminate on the $^{207}Pb/^{204}Pb$ versus $^{206}Pb/^{204}Pb$ plot, 1.098 ± 0.189 on $^{208}Pb/^{206}Pb$ versus $^{206}Pb/^{204}Pb$ plot, and 0.170 ± 0.010 on the ($^{208}Pb/^{206}Pb \times 10$) versus ($^{207}Pb/^{206}Pb \times 100$) plot. The slopes $\pm$ error at 95 percent confidence level were determined by a model-2 Yorkfit (Ludwig, 1993, after York, 1969). These lines, marked "dt," are drawn in Figure 5a to d.

Potential causes of line and model slopes

Potential causes of the slopes in the linear distributions of the galena lead isotope data from the Buttle Lake ore lenses are examined by three general models summarized in Table 4: (1) evolution of lead isotope ratios over time in an orogen (or), (2) mixing of variably leached radiogenic components from older basement rocks (lv), and (3) mixing of isotopically distinct mantle and upper crustal lead (mx).

Evolution of lead within the orogen or island arc over time would yield linear data arrays with slopes of 0.038, 1.154, and 0.115 in Figure 5a to c, respectively (Table 4: orogen growth curve, or; Fig. 6). These slopes are approximately tangent to the orogen growth curve of Zartman and Doe (1981, as tabulated in Godwin et al., 1988). Because the slopes are based on a specific model, an error in slope cannot be defined. Lines of this slope are marked "or" in the plots (Fig. 5a–c).

Differences in lead isotope composition due to selective leaching of old basement are not easily assessed. However, it is known that partial leaching of older rocks can selectively extract a relatively radiogenic lead component (cf. Doe and Delevaux, 1972). Uranogenic lead (^{206}Pb and ^{207}Pb) and thorogenic lead (^{208}Pb) generally is leached readily because it resides close to original uranium or thorium sites that can have been damaged by radioactivity. On the other hand, lead from the major lead-bearing minerals in rocks, feldspars, and sulfides would tend to remain in the source. Thus, selective leaching can produce linear data arrays that extend to relatively radiogenic composition, as noted in some carbonate-hosted deposits and in some intrusion-related vein systems (Heyl, 1969; Heyl et al., 1974; Godwin et al., 1982; Crocetti

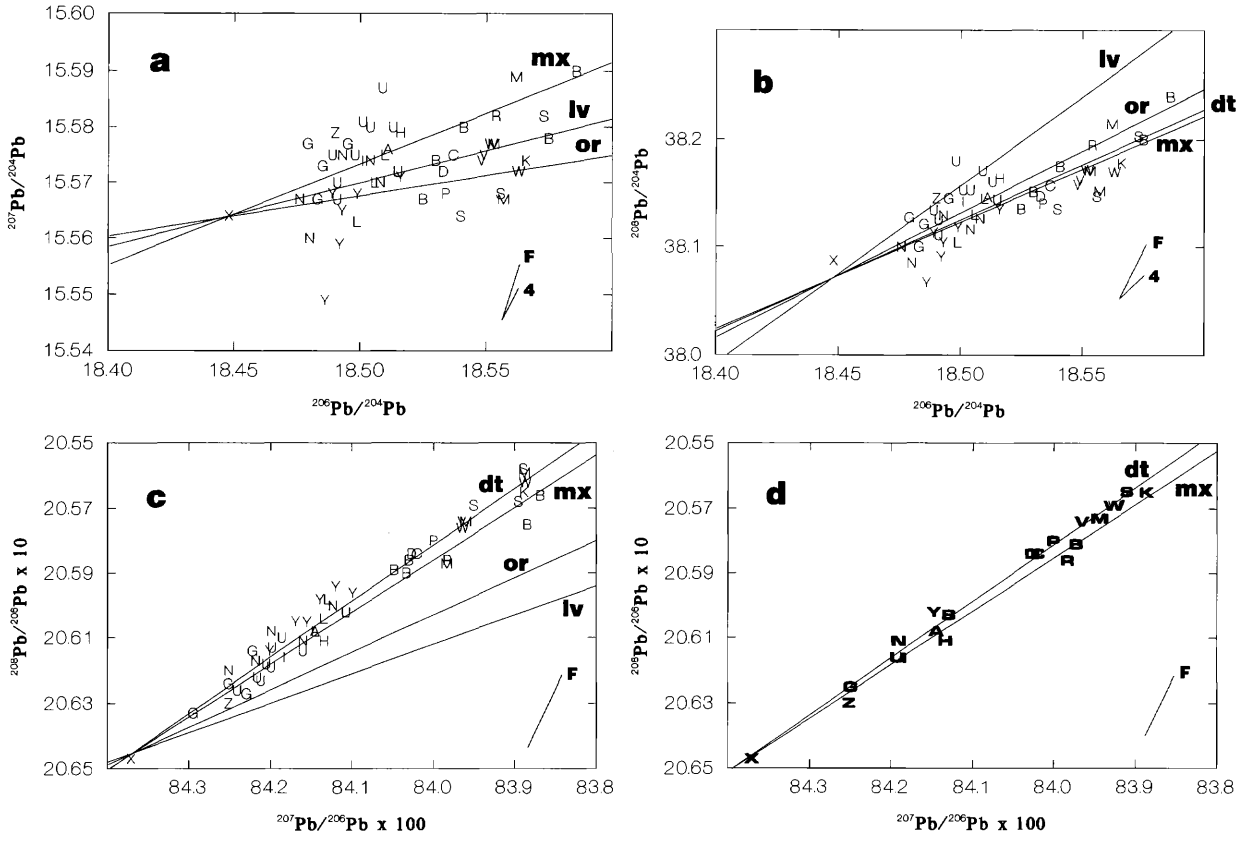

FIG. 5. Small-scale galena lead isotope plots for the Buttle Lake mining camp, southwestern British Columbia. Data and symbols for (a) to (c) are given in Table 2, and in Table 3 for (d). (a). $^{207}Pb/^{204}Pb$ versus $^{206}Pb/^{204}Pb$ plot. (b). $^{208}Pb/^{204}Pb$ versus $^{206}Pb/^{204}Pb$ plot. (c) and (d). ($^{208}Pb/^{206}Pb \times 10$) versus ($^{207}Pb/^{206}Pb \times 100$) plots. Table 4 and Figure 5 define slopes and errors of lines representing: (1) the ore lens data (dt), (2) orogen growth (or) and selective leaching of older footwall rocks (lv), and (3) mantle-upper crust mixing (mx). Lines that do not model the data are drawn from the x axis value for the ore clast breccia (X) so that the slopes can be compared. The line through the data (dt) in (c) and (d) is only close in slope to the mantle-upper crust mixing vector (mx). The slopes for orogen growth (or) and selective leaching (lv) do not follow the data (dt) trend. F = trend of fractionation error; 4 = trend of ^{204}Pb error. Data trends parallel these errors in a and b. However, this error elongation is not apparent in c and d, which eliminate the ^{204}Pb error.

TABLE 4. Calculated Slopes for Lead Isotope Plots to Test Model Concepts (lines corresponding to slopes below are plotted in Fig. 5A–D)

Models	$^{207}Pb/^{204}Pb$ vs. $^{206}Pb/^{204}Pb$ (Fig. 5A) Slope[1] ± error[1] (95%)	$^{206}Pb/^{204}Pb$ vs. $^{206}Pb/^{204}Pb$ (Fig. 5B) Slope[1] ± error[1] (95%)	($^{206}Pb/^{206}Pb \times 10$) vs. ($^{207}Pb/^{206}Pb \times 100$) (Fig. 5C and D) Slope[1] ± error[1] (95%)
Buttle Lake camp ore lenses (dt)[2]	Indeterminate ± indeterminate	1.098 ± 0.189	0.170 ± 0.010
Orogen growth[3] (or)	0.038 ± indeterminate	1.154 ± indeterminate	0.115 ± indeterminate
Leaching of older basement: assumed to be analogous to galena lead isotope ratios associated with silver-rich veins related to Cretaceous plutons[4] (lv)	0.119 ± 0.018	1.616 ± 0.160	0.095 ± 0.025
Mantle-upper crust mixing[5] (mx)	0.184 ± indeterminate	1.010 ± indeterminate	0.161 ± indeterminate

[1] Slope and errors (at 95% confidence level) were calculated using a model-2 Yorkfit and ISOPLOT after Ludwig (1993; York, 1969); errors for the slopes of lines calculated from the plumbotectonic models of Zartman and Doe (1981) are indeterminate

[2] Average slope through data of Table 2; lines of this slope in Figure 5b to d are marked "dt"; a model-2 Yorkfit cannot be determined on the $^{207}Pb/^{204}Pb$ vs. $^{206}Pb/^{204}Pb$ plot of Figure 5a

[3] Average slope of orogen growth curve (after Zartman and Doe, 1981, as tabulated in Godwin et al., 1988) from the base of the Devonian (0.41 Ga) to the base of the Triassic (0.25 Ga); lines of this slope in Figure 5a to d are marked "or"

[4] Estimated slopes calculated from data for silver-rich veins associated with Cretaceous plutons (Godwin et al., 1982); lines of this slope in Figure 5a to d are marked "lv"

[5] Mean of mixing-line slopes for the Devonian (0.41 Ga), the Carboniferous (0.36 Ga), and the Permian (0.29 Ga); slopes are calculated for mixing lines between the growth curves defined by Zartman and Doe (1981); lines of this slope in Figure 5a to d are marked "mx"

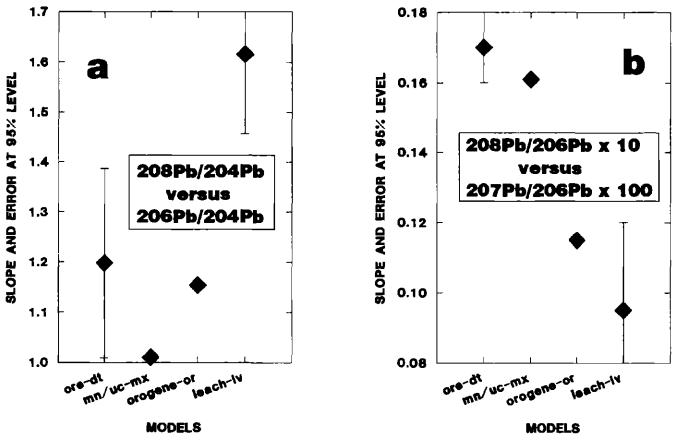

FIG. 6. Comparison of model slopes and associated errors (95% level) from Table 4. (a) and (b). $^{208}Pb/^{204}Pb$ versus $^{207}Pb/^{204}Pb$ plots and ($^{208}Pb/^{206}Pb \times 10$) versus ($^{207}Pb/^{206}Pb \times 100$) plots, respectively. The slope for ore lens data in the $^{207}Pb/^{204}Pb$ versus $^{206}Pb/^{204}Pb$ plot is indeterminate. Abbreviations: ore-dt = ore lens data, orogen-or = orogen growth, leach-lv = selective leaching of older basement units, mn/uc-mx = mantle-upper crust mixing.

et al., 1988; Robinson and Godwin, 1996). The slope of a linear array produced in such a manner does not relate directly to age. The line is a mixing line extending from normally generated lead isotopes and lead isotopes produced directly from uranium and thorium (without ^{204}Pb). In general, these lines tend to be tangential to growth curves; consequently, they tend to have similar slopes over time blocks as large as the Devonian to Cretaceous examined here. Data for Cretaceous intrusion-related silver-rich vein systems (Godwin et al., 1982), mainly from the Yukon Territory, form a linear data array to markedly radiogenic values. The slopes of these data are used here as a first approximation to evaluation of the effect of selective leaching of old basement at the Buttle Lake camp. The slopes and errors (Table 3: model-2, Yorkfit; Fig. 6) on these lines are: 0.119 ± 0.018, 1.616 ± 0.160, and 0.095 ± 0.025 in Figure 5a to c, respectively. They are marked "lv" on these plots.

Mantle-upper crustal mixing

Mixing of variable amounts of lead between the mantle and upper crust should cause the data to form linear arrays that have slopes close to 0.184, 1.010, and 0.161 in Figure 5a to c, respectively (Table 4: mantle-upper crust mixing model; Fig. 6). Because the slopes are based on a specific model, an error in the slope cannot be defined. Lines of this slope are marked "mx" in Figure 5a to d.

Comparison of model slopes

Slopes for the three models tested (mantle-upper crust = mx, orogen = or, and selective leaching of old basement = lv) are compared to the slope of data from the Buttle Lake camp ore lenses (dt) in Table 4 and Figures 5a to d, and 6. Figure 6 shows that of the models tested, only the slope derived from mantle-upper crustal mixing (mx) is consistently close to the ore lens data (dt). The best discriminator of the differences in slope between the three models is on the ($^{208}Pb/^{206}Pb \times 10$) versus ($^{207}Pb/^{206}Pb \times 100$) plot (Table 4, Figs. 5c–d, and 6).

The slope of orogen growth (or) is distinctly flatter than the ore lens data trend (dt) in Figure 5c and d (Table 4: 0.115 versus 0.170 ± 0.010; Fig. 6). Therefore, lead evolution through time does not appear to explain the linear distribution of data. Another reason that the variation in lead isotopes among the lenses cannot represent time differences is that galena lead isotope data overlap from ore lenses in ore-bearing units that are both stratigraphically lowest (Table 2 and Fig. 3: H-W horizon) and highest (Table 2 and Fig. 3: Lynx-Myra-Price horizon).

The slope related to selective leaching of older basement (lv) is distinctly different from the ore lens data trend (dt) in Table 4, and in Figures 5b to d and 6. It is steeper in Figures 5b and 6 (Table 4: 1.616 ± 0.160 versus 1.098 ± 0.189), but shallower in Figures 5c, d, and 6 (Table 4: 0.095 ± 0.025 versus 0.170 ± 0.010).

Definition of End-Member Lead Isotope Compositions

Differences in galena lead isotope ratios exist among ore lenses in the Buttle Lake mining camp. In Table 3, the average galena lead isotope ratio for each lens is ranked from least (rank 1) to most (rank 20) radiogenic values, as measured along the line representing the trend of the data (dt) in Figure 5d. Table 5 summarizes the stratigraphic position (H-W versus Lynx-Myra-Price) and host-rock spatial affiliations for each of the ore lenses. Inspection of Figure 5d and Table 5 shows that a spatial relationship exists between the lead isotope compositions of the ore lenses and the compositions of the host and footwall rocks.

Least radiogenic galena lead

The least radiogenic galena lead analysis is from a sulfide fragment in the ore clast breccia (Tables 3 and 5, Fig. 5a–d: X). A significant feature of the ore clast breccia is that it contains olistoliths of pyrite-mineralized rhyolite tuffs. Many of the olistoliths contain semimassive to massive sulfide + barite + quartz pods. Therefore, mineralization and the source of lead appears to be closely associated with rhyolite. Lead isotope ratios from galena in the ore clast breccia anchor the less radiogenic end of the linear array in Figure 5 and appear to reflect an end-member rhyolite composition.

Most radiogenic galena lead

Lenses with notably radiogenic leads in the H-W horizon (Table 3 and Fig. 5d) are H-W North (K: the most radiogenic, rank 20), H-W Main (M, rank 17), and Battle Main (B, rank 15). Similarly radiogenic leads in the Lynx-Myra-Price horizon (Table 3 and Fig. 5d) are Lynx S (S: the second most radiogenic, rank 19) and Lynx West G (W, rank 18, and V, rank 16).

The H-W North (K), H-W Main (M), and Battle Main (B) lenses are underlain by an intensely altered discharge stockwork in the Price formation andesite. The radiogenic Lynx S (S) lens overlies, or is within, a strongly altered discharge stockwork, stringer zone in 5E andesite. Lynx West G lenses (V and W) lie on top of rhyolitic tuffs but do not have distinctive feeder zones. The tuffs probably served as conduits for mineralizing fluids channeled laterally from al-

TABLE 5. Horizon[1] and Host-Rock Affiliations with Ore Lenses, Buttle Lake Mining Camp, Southwestern British Columbia

Rank order (from Fig. 5d)	Lens or zone (Tables 4 and 5)	Horizon position[1]	Symbol (Figs. 2 and 3)	Associated units (Fig. 3)	End-member affiliation	Comments
1	Ore clast breccia	unknown	X	Ore clast breccia	Rhyolite	Possible end member
2	Hanging wall	H-W	Z	Quartz-feldspar porphyry hanging-wall andesite	Rhyolite	Possible near end member
3	Gap	H-W	G	Quartz porphyritic rhyolite Price formation (?)	Rhyolite	Possible near end member
4	Battle Upper	H-W	U	Rhyolite volcaniclastics	Rhyolite	Possible near end member
5	Lynx (I)	Ore-X	I	Ore clast breccia	Rhyolite	Possible near end member
6	H-W North Bornite	H-W	N	Rhyolite volcaniclastics	Rhyolite	
7	H-W Upper (A)	H-W	A	Rhyolite volcaniclastics	Rhyolite	
8	Lynx (H)	Ore-X	H	Ore clast breccia (?)	Rhyolite	
9	Myra	L-M-P	Y	Lynx-Myra-Price horizon	Rhyolite	
10	Battle Main	H-W	B	Price formation	Andesite	Immediately above discharge stockwork in Price formation
11	H-W Upper (D)	H-W	D	Rhyolite volcaniclastics	Rhyolite	
12	H-W Upper (C)	H-W	C	Rhyolite volcaniclastics	Rhyolite	
13	Price	L-M-P	P	Lynx-Myra-Price horizon Lower mafic volcanics	Rhyolite Andesite	
14	Ridge West	H-W	R	Rhyolite volcaniclastics	Rhyolite	
15	Battle Main	H-W	B	Price formation	Andesite	Immediately above discharge stockwork in Price formation
16	Lynx West G (V)	L-M-P	V	Lynx-Myra-Price horizon 5E andesite	Rhyolite Andesite	
17	H-W Main	H-W	M	Price formation	Andesite	Immediately above discharge stockwork in Price formation
18	Lynx West G (W)	L-M-P	W	Lynx-Myra-Price horizon 5E andesite	Rhyolite Andesite	
19	Lynx S	L-M-P	S	Lynx-Myra-Price horizon 5E andesite	Rhyolite Andesite	Immediately above discharge stockwork in SE andesite
20	H-W North (K)	H-W	K	Price formation	Andesite	Immediately above discharge stockwork in Price formation; possible end member

[1] Mine nomenclature uses "horizon": H-W = H-W horizon; L-M-P = Lynx-Myra-Price horizon; Ore-X = Ore clast breccia

tered underlying andesites (Juras, 1987). Thus, the most radiogenic lead isotope signatures are from lenses that are underlain mainly (or indirectly in the case of Lynx West) by andesitic and/or dacitic rocks. In particular, the H-W North (K) lens appears to represent a spatial association with an end-member andesite of the Price formation (Tables 3 and 5).

Intermediate and variable galena lead

Deposits that plot between rhyolite and andesite end members are associated with a footwall composed of (1) rhyolite, (2) andesite, dacite, and associated sedimentary rocks, or (3) a mixture of (1) and (2). Within the H-W horizon, the Battle Upper (Table 5: U, rank 4), Ridge West (R, rank 14), and H-W Upper (A, rank 7, C, rank 12, and D, rank 11) zones have an immediate footwall consisting of a 30- to 75-m-thick unit of rhyolitic tuff that overlies the Price formation. The Lynx H and I (H, rank 8, and I, rank 5), Myra (Y, rank 9), and Price (P, rank 13) lenses of the Lynx-Myra-Price horizon are underlain by altered rhyolite clastics that overlie dacite volcaniclastic deposits of the upper dacite unit and/or andesite-dacite clastic deposits of the lower mixed volcaniclastic unit.

Galena with highly variable lead isotope analyses occur within some lenses. In the Battle Main (B, ranks 10 and 15), H-W Upper (A, rank 7, versus C, rank 12, and D, rank 11), and H-W North (N, rank 6, and K, rank 20) lenses galena lead isotope results plot in both of the apparent clusters (Tables 3 and 5, Fig. 5). This indicates that some ore lenses may have been generated complexly in several stages from varied fluid sources. Mixing of lead isotopes by leaching of lead from previously formed deposits may have occurred in some cases.

Discussion

Lead isotope data can be used to constrain hypotheses about the source of lead and other metals in mineralized districts. For example, lead isotope compositions for galena in kuroko deposits in the Hokuroku district of Japan (Fehn et al., 1983) differ among deposits, and also differ between yellow and black ores within deposits. Fehn et al. (1983) suggested that the shifts in the lead isotope ratios among deposits are due to varied footwall sources of the lead during evolution of the hydrothermal systems related to ore deposition. Similar explanations for shifts in isotopic ratios among volcanogenic massive sulfide deposits in Tasmania, Australia, have been made by Gulson and Porritt (1989). Extremely radiogenic lead values are well known in carbonate-hosted deposits and pluton-associated silver-rich veins (e.g., Heyl, 1969; Heyl et al., 1974; Godwin et al., 1982; Crocetti et al., 1988). In many of these cases, mineralizing fluids probably

traveled through sandstone aquifers or layers that contained concentrations of zircon. The markedly radiogenic character of the lead isotopes commonly appears to arise from selective leaching of radiogenic-rich lead that is ^{204}Pb poor from zircon (and/or other minerals that contain uranium and thorium).

There are two general sources of metals for volcanogenic deposits: magmatic fluids and/or the metals leached from footwall rocks (Stanton, 1990, 1991). Crystallizing magmas can evolve a hydrous phase that is rich in metals (Whitney, 1989). Corliss (1971) proposed that hot, convecting seawater leached metals from volcanic glass in the subsea-floor volcanic pile. These fluids, when exhaled onto the sea floor, formed stratiform deposits. A hybrid process involving leaching and magmatic processes has been proposed by Sawkins and Kowalik (1981) and adopted by Stanton (1990, 1991); they suppose the operation of relatively long-lived seawater convection systems on which are superimposed pulses of metal-rich magmatic fluids.

Following the hybrid model of Sawkins and Kowalik (1981), it is argued that lead is leached from within and below the mine stratigraphic sequence, with a possible contribution of lead from a devolatilizing felsic magma chamber. Lead isotope data in galena from the Buttle Lake mining camp define a trend that can be described as a mixing line between rhyolite and andesite end-member signatures. This trend does not relate to age differences among the ore lenses, but it appears to mimic varied mixing of upper crustal and mantle components. Mixing of variable proportions of lead from upper crust and mantle sources would produce data with slope mx. The trend of the data (dt) in Figure 5 (Fig. 6) is similar to this trend.

The variation in upper crustal and mantle components could be due to original differences in the lead isotope signature of the andesite and rhyolite. Lead hydrothermally leached from these rocks (and/or from magmatic fluids) could mix and define the line between the end-member compositions. On the other hand, the andesite and rhyolite could have had similar isotopic signatures and the radiogenic component could have been extracted from pelagic or continental upper crustal sediments, mainly within the andesite packages (cf. Smith, 1993). Below, we discuss these two conceptual models of mantle-upper crust lead isotope mixing between: andesite and rhyolite (Fig. 7a), and volcanics and oceanic sediments (Fig. 7b).

Isotopic mixing between andesite and rhyolite

The end members in the mantle-upper crust mixing trend in lead isotopes of galena could be isotopically distinct rhyolitic magmas and/or resultant rocks, and andesitic magmas and/or resultant rocks (Fig. 7a). Differences in lead isotope compositions of volcanic rocks have been correlated with different magma type by Dupre and Echeverria (1984). In the Buttle Lake camp, the most obvious candidates, by reference to Table 5, are a rhyolite source for the relatively primitive lead, and an andesite source for the relatively radiogenic lead. The implication is that the rhyolite and andesite are not genetically related directly and that their source magmas were contaminated variably by subduction of sediment with an upper crustal lead isotope signature. One lead isotope analysis of andesite and seven analyses of rhyolite, reported in Andrew and Godwin (1989), are unable to resolve whether or not there are initial isotope differences between these units.

Andesitic units of the Price formation and the Myra formation (Fig. 3: hanging-wall andesite, fragments in the ore clast breccia, fragments in the lower mixed volcaniclastic rocks, and upper dacite-5E andesite) are enriched in Nd and P compared to normal-type midocean ridge basalts; this may indicate contamination by a subducted sediment component (Juras, 1987). Rhyolite rocks in the H-W and Lynx-Myra-Price horizons contain low total rare earth element abundances, low concentrations of high field strength elements, and a depletion trend in heavy rare earth elements. Juras (1987) argued that these patterns are consistent with partial melting of island-arc tholeiitic basalt or basaltic andesite. Thus, the available lithogeochemical data are consistent with fundamentally different magma origins for the rhyolite and andesite. The primitive rhyolite is relatively uncontaminated with an upper crustal isotopic lead component compared to andesite.

Ore lenses that are most closely associated spatially with rhyolite contain isotopically relatively primitive lead. These include the sulfide fragments in the ore clast breccia (Table 5: X), the Gap lens (G), the Battle Upper zone lens (U), the H-W North Bornite zone lens (N), the Myra lens (Y), and the Lynx H and I lenses (H, I). Lenses of this type are characterized by a zinc-, barite-, and lead-rich, but relatively copper-poor, metal association that is typical of rhyolite-associated syngenetic mineralization (Stanton, 1991, 1990). Ore lenses with the most radiogenic lead include: H-W North (K), the Battle Main lens (B), the H-W Main lens (M), and the Lynx S lens (S). Lenses of this type overlie discharge stockworks in andesitic volcanic rocks and associated sedimentary rocks; they are relatively copper and zinc rich, but lead and barite poor. This metal assemblage is typical of syngenetic mineralization that overlies andesite (Stanton, 1991, 1990).

Isotopic mixing between volcanics and oceanic sediments

Isotopic mixing between volcanic and oceanic sedimentary rocks, a mixed provenance model (Fig. 7b), would yield the same slope in the data (Figs. 5 and 6, mx). However, in this case pelagic or continental sediments interbedded with the andesitic units are considered to have been significant sources of lead. Such sediments would normally have an upper crustal signature and could be a source of radiogenic lead. The rhyolitic units do not contain notable quantities of such units, and therefore, fluids that emanate from or through them would be less radiogenic. Differences in isotopic compositions of rhyolite versus andesite could be insignificant compared to the differences between the volcanic rocks and pelagic and/or continental sediments.

The main difficulty with the mixed provenance model is the paucity of pelagic or continental sedimentary rocks in the Buttle Lake camp basin. In the explored upper 300 m of the Price formation, only about 5 percent consists of sedimentary units. Furthermore, these sedimentary rocks consist mainly of volcaniclastic material with only minor shales. Similarly, most sedimentary rocks in the Myra formation are also volcanic rather than oceanic sedimentary in origin. Sedimentary units, however, could occur in significant volumes in the Price

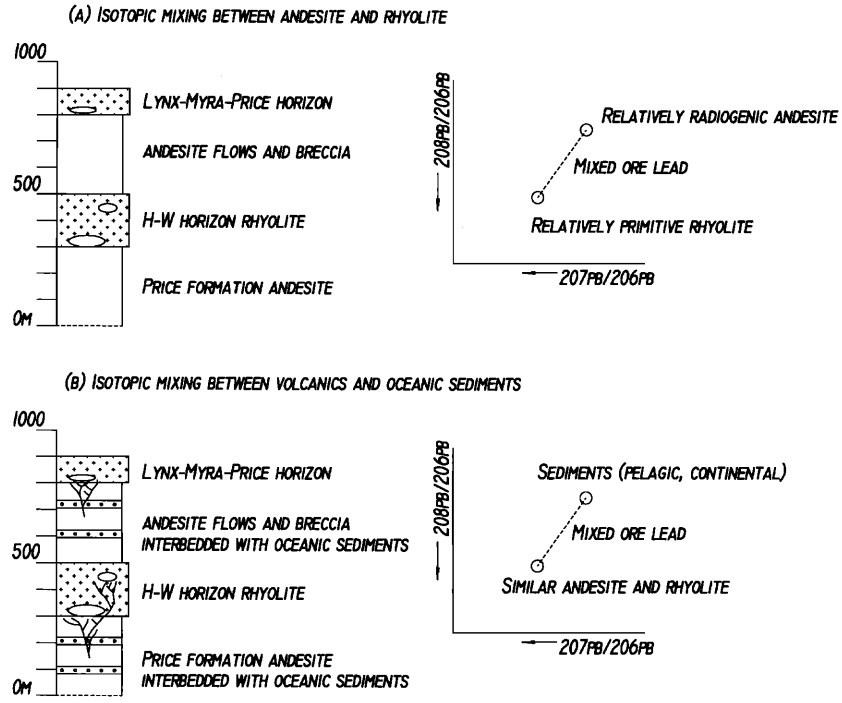

FIG. 7. Two models that can explain the orogen-upper crust mixing line trend (mx) in galena lead isotopes from the ore lenses in the Myra formation, Buttle Lake mining camp. (a). Mixing line trend (mx) produced by leaching and/or magmatic fluid component of end-member volcanic rocks with distinctive lead isotope signatures, namely, relatively nonradiogenic rhyolite and relatively radiogenic andesite. (b). Mixing line trend (mx) produced by leaching from volcanic rocks with a similar relatively nonradiogenic lead isotope signature, but with addition of relatively radiogenic lead from interbedded oceanic, pelagic, and/or continentally derived sediments that have a characteristically upper crustal lead isotope signature.

formation at depth; they could also occur in unknown lower units.

A Genetic Model for Mineralization in the H-W Horizon

Mineralization occurs at three levels within the H-W horizon:

1. The largest massive sulfide lenses, namely the H-W Main lens (Fig. 3: M), the H-W North lens (K), the H-W North Bornite lens (N), and the Battle Main zone lens (B) occur at the Price formation contact.
2. Upper zone massive sulfide lenses, represented by the H-W Upper zone lenses (A, C, and D), the Ridge West zone lens (R), and the Battle Upper lens (U), occur within or above a 5- to 50-m-thick package of rhyolitic tuff (Robinson, 1994).
3. Hanging-wall zone massive sulfide deposits occur above the rhyolite flow dome complex and below the hanging-wall andesite.

The positions of the Gap (G) and H-W North Bornite (N) lenses are variable, occurring close to the Price formation contact in some regions but separated from the Price formation with up to 70 m of rhyolite tuffaceous deposits in other areas. They therefore are stratigraphically similar to the H-W North Bornite lens.

The mineralizing system evolved penecontemporaneously with the onset of felsic volcanism. The following sequence of events, following the upper crust-mantle lead isotope mixing model (Fig. 7), is envisioned:

1. Andesitic arc volcanism is represented, at least in part, by the Price formation andesite. A rift basin was developed within the Price formation (Juras, 1987). Mineralization was penecontemporaneous with subsidence and active block faulting. In such extensional regimes, seismic pumping processes may have channeled fluids toward the surface (Sibson et al., 1975; cf. Russell, 1978, 1983; cf. Cathles, 1993). This is compatible with the observed close spatial relationship of many stratiform deposits to fault zones and to steeply dipping fracture systems (LeHuray et al., 1987; Gibson and Kerr, 1992; Large, 1992).
2. Hydrothermal convection cells within the andesitic footwall (cf. Cathles, 1993) leached lead and other metals from the footwall for subsequent deposition within ore lenses above discharge stockworks. A contribution of fluid from a mafic or andesitic magma chamber cannot be discounted. The largest deposits, H-W Main (M), H-W North (K), and Battle Main (B: Tables 3 and 5: rank 17, 20, and 15, respectively), are characterized by relatively radiogenic lead. This is compatible with leaching of andesite with a relatively radiogenic lead isotope composition (with or without a magmatic fluid component from an andesitic magma chamber), or with mixing of relatively primitive lead isotopes leached from volcanics with radiogenic lead leached from oceanic sediment (Smith, 1993).
3. A felsic volcanic regime developed contemporaneously to one side of the rifted basin. A contribution of lead and other metals by magmatic fluids could have shifted the lead

isotope values toward the relatively primitive end-member composition. The most primitive lead is associated with sulfide fragments in the ore clast breccia (Table 5: rank 1). The ore clast breccia (Fig. 3: X) contains fragments of H-W horizon lithologies, including olistoliths of pyrite-mineralized rhyolitic tuffs. Many of the olistoliths contain semimassive to massive sulfide + barite + quartz pods. The mineralization is similar in nature to that of upper or hanging-wall lenses, but the relatively primitive lead isotope signature suggests a greater contribution of metals from the rhyolite itself. Both the Gap (G) and the hanging-wall (Z) massive sulfide lenses plot near the primitive end-member (Fig. 6; Table 5: rank order 2 and 3, respectively). The felsic unit that locally occurs with the Gap lens might reflect an appropriate source. The Battle Main lens (B) has an intermediate lead component (Table 5: rank 9). Contributions from both andesite and rhyolite provinences might be implied.

4. H-W horizon volcaniclastic rocks, consisting of fine rhyolitic tuffaceous deposits through to rhyolitic tuffaceous sedimentary rocks, were deposited (Robinson, 1994). Extension and subsidence of the Buttle Lake camp basin continued and faults propagated upward through the rhyolite volcaniclastic package. The faults formed conduits for fluids that deposited upper zone massive sulfide deposits (see below).

5. Upper zone massive sulfide lenses, including the H-W Upper (Fig. 3: A, C, and D), Ridge West (R), and Battle Upper (U) lenses, were deposited above the rhyolite volcaniclastic rocks. The upper zone lenses are underlain by polymetallic stockworks in volcaniclastic units but occur above the Main lens trend (H-W Main, Battle Main). It is reasonable to envision that hydrothermal fluids continued to circulate upward through the main lenses and leached some metals from the overlying volcaniclastic package prior to depositing the upper zone lenses. The resulting upper zone mineralization consequently would have the mixed lead isotope signature observed.

6. Intrusion of quartz porphyritic rhyolite into the Price andesite and rhyolite pyroclastic rocks as a hot, shallow-level sill marked the transition from explosive to effusive volcanism (Robinson, 1994). Extrusion of the quartz-feldspar porphyritic rhyolite and the green quartz-feldspar porphyritic rhyolite flows ended the felsic eruptive cycle. Continued basin extension and propagation of faults upward through the rhyolite flow dome complex allowed fluids to migrate upward to deposit the hanging-wall zone massive sulfide lenses.

Conclusions

Lead isotope data for galena from the Buttle Lake mining camp indicate that lead evolved in an orogen or island-arc environment. There is a pronounced linear trend in the lead isotope data that can be explained as a mixing line. Positions of data along this trend do not relate to age differences among the ore lenses or to variable selective leaching of lead isotope components from significantly older footwall source rocks. However, the line appears to represent one or a combination of variable mixing of lead from felsic and andesitic rocks (or related magmatic fluids), each with distinctly different proportions of upper crustal and mantle lead isotopes; or mixing of lead isotopes from relatively radiogenic oceanic sediment with relatively primitive lead isotopes from the volcanic rocks (or related magmatic fluids).

Galena lead isotope ratios can be used to help prioritize exploration for ore lenses throughout the Buttle Lake mining camp. In the H-W horizon, markedly radiogenic lead is characteristic of deposits that lie immediately above the Price formation contact. Since lenses in this trend are among the largest, they are the most attractive exploration target. Comparatively primitive lead isotope signatures are characteristic of lenses that are associated with rhyolite in the footwall or of lenses that may have had a contribution of lead from magmatic fluid from a rhyolite source. Lenses of this type appear to be smaller than those in the Main lens trend, but they can be comparatively enriched in precious and base metals. The sample from the ore clast breccia contains mineralized rhyolite clasts and has a markedly primitive lead isotope composition compared to data from other lenses. The implication is that the breccia may have been derived from lenses closely related to rhyolite volcanism; these lenses remain to be discovered.

Acknowledgments

We thank Westmin Resources Limited for access to company data, payment of the analytical costs for some of the samples, and permission to publish. A.J. Sinclair, Department of Geological Sciences, University of British Columbia, is thanked for an early critical review of the manuscript. J.F.H. Thompson and T. J. Barrett of the Mineral Deposit Research Unit (MDRU) of University of British Columbia provided helpful suggestions. Two reviews for *Economic Geology* substantially helped the manuscript. A. Hamilton collected some of the samples from the Battle zone. Galena lead isotope analyses were done by A. Pickering at the Geochronometry Laboratory, Department of Geological Sciences, University of British Columbia. Funding to C.I. Godwin was provided by a Natural Sciences and Engineering Research Council (Canada) operating grant. Financial support for M. Robinson was from Westmin Resources Limited, the Volcanogenic Massive Sulfide project of MDRU, the F.J. Nicholson scholarship, and a Shell Canada scholarship. MDRU is funded by the Natural Sciences and Engineering Research Council of Canada, the Science Council of British Columbia, and ten mining and exploration member companies. These industry partners are Granges Inc., Homestake Canada Inc., Inco Exploration Ltd., Technical Services Inc., Kennecott Canada Inc., Lac Minerals Ltd., Metall Mining Corporation, Placer Dome Ltd., Teck Corporation, and Westmin Resources Ltd. (industry project leader).

July 21, 1994; February 14, 1996

REFERENCES

Andrew, A., 1987, Lead and strontium isotope study of five volcanic and intrusive rock suites and related mineral deposits, Vancouver Island, British Columbia: Unpublished Ph.D. thesis, Vancouver, University of British Columbia, 254 p.

Andrew, A., and Godwin, C.I., 1989, Lead and strontium isotope geochemistry of the Paleozoic Sicker Group and Jurassic Bonanza Group volcanic rocks and island intrusions, Vancouver Island, British Columbia: Canadian Journal of Earth Sciences, v. 26, p. 894–907.

Barrett, T.J., Sherlock, R.L., Juras, S.J., Wilson, G.C., and Allen, A., 1994, Geological investigations of the H-W Deposit, Buttle Lake camp, central Vancouver Island: British Columbia Ministry of Energy, Mines and Petroleum Resources Paper 1994–1, p. 339–344.

Bates, R.L., and Jackson, J.A., eds., 1987, Glossary of geology 3rd ed.: Alexandria, VA, American Geological Institute, 788 p.

Brandon, M.T., Orchard, M.J., Parrish, R.R., Sutherland Brown, A., and Yorath, C.J., 1986, Fossil ages and isotopic dates from the Paleozoic Sicker Group and associated intrusive rocks, Vancouver Island, British Columbia: Canada Geological Survey Paper 86–1A, p. 683–696.

Cathles, L.M., 1993, A capless 350°C flow zone model to explain megaplumes, salinity variations, and high-temperature veins in Ridge axis hydrothermal systems: ECONOMIC GEOLOGY, v. 88, p. 1933–1976

Cathles, L.M., Guber, A.L., Lenagh, T.C., and Dudás, F.Ö., 1983, Kuroko-type massive sulfide deposits of Japan: Products of an aborted island-arc rift: ECONOMIC GEOLOGY MONOGRAPH 5, p. 96–114.

Corliss, J.B., 1971, The origin of metal-bearing submarine hydrothermal solutions: Journal of Geophysical Research, v. 76, p. 8128–8138.

Craig, H., 1969, Geochemistry and origin of the Red Sea brines, *in* Degens, E.T., and Ross, D.A., eds., Hot brines and recent heavy metal deposits in the Red Sea: Springer-Verlag, New York, p. 209–242.

Crocetti, C.A., Holland, H.D., and McKenna, L.W., 1988, Isotopic composition of lead in galenas from Viburnum Trend, Missouri: ECONOMIC GEOLOGY, v. 83, p. 355–376.

Doe, B.R., and Delevaux, M.H., 1972, Source of lead in southeast Missouri galena ores: ECONOMIC GEOLOGY, v. 67, p. 409–425.

Doe, B.R., and Zartman, R.E., 1979, Plumbo-tectonics 1, the Phanerozoic, *in* Barnes, H.L., ed., Geochemistry of hydrothermal ore deposits, 2nd edition: New York, Wiley Interscience, p. 22–70.

Dupre, B., and Echeverria, L.M., 1984, Pb isotopes of Gorgona Island (Colombia): Isotopic variations correlated with magma type: Earth and Planetary Science Letters, v. 67, p. 186–190.

Fehn, U., Doe, B.R., and Delevaux, M.H., 1983, The distribution of lead isotopes and the origin of kuroko ore deposits in the Hokuroku district, Japan: ECONOMIC GEOLOGY MONOGRAPH 5, p. 488–506.

Fyles, J.T., 1955, Geology of the Cowichan Lake Area, Vancouver Island, British Columbia: British Columbia Ministry of Energy, Mines and Petroleum Resources Bulletin 37, 72 p.

Gibson, H.L., and Kerr, D.J., 1992, Giant volcanic-associated massive sulphide deposits with emphasis on Archean examples, *in* Whiting, B.H., Mason, R., and Hodgson, C.J., eds., Giant ore deposits: Kingston, Queen's University, p. 492–522.

Godwin, C.I., Sinclair, A.J., and Ryan, B.D., 1982, Lead isotope models for the genesis of carbonate-hosted Zn-Pb, shale-hosted Ba-Zn-Pb, and silver-rich deposits in the northern Canadian Cordillera: ECONOMIC GEOLOGY, v. 77, p. 82–94.

Godwin, C.I., Gabites, J.E., and Andrew, A., 1988, LEADTABLE: A galena-lead isotope database for the Canadian Cordillera, with a guide to its use by explorationists: British Columbia Ministry of Energy, Mines and Petroleum Resources Paper 1988–4, 188 p.

Gulson, B.L., and Porritt, P.M., 1987, Base metal exploration of the Mount Read volcanics, western Tasmania: Pt. II. Lead isotope signatures and genetic implications: ECONOMIC GEOLOGY v. 82, p. 291–307.

Heyl, A.V., 1969, Some aspects of zinc-lead-barite-fluorite deposits in the Mississippi Valley, U.S.A.: Institution of Mining and Metallurgy Transactions, v. 78, section B, p. B148-B160.

Heyl, A.V., Landis, G.P., and Zartman, R.E., 1974, Isotopic evidence for the origin of Mississippi Valley-type mineral deposits: A review: ECONOMIC GEOLOGY, v. 69, p. 992–1006.

Jeffery, W.G., 1970, Buttle Lake: British Columbia Ministry of Energy, Mines and Petroleum Resources Miscellaneous Open File Report, map with notes.

Jones, D.L., Siberling, N.J., and Hillhouse, J., 1977, Wrangellia–a displaced terrane in northwestern North America: Canadian Journal of Earth Sciences, v. 14, p. 2565–2577.

Juras, S.J., 1987, Geology of the polymetallic volcanogenic Buttle Lake camp, with emphasis on the Price hillside, central Vancouver Island, British Columbia, Canada: Unpublished Ph.D. thesis, Vancouver, University of British Columbia, 277 p.

Juras, S.J., and Pearson, C.A., 1990, Mineral deposits of the southern Canadian Cordillera: Geological Association of Canada-Mineralogical Association of Canada Joint Meeting, Vancouver, BC, 1990, Guidebook for field trip B2, p. 1–21.

Large, R.R., 1992, Australian volcanic-hosted massive sulfide deposits: Features, styles, and genetic models: ECONOMIC GEOLOGY, v. 87, p. 469–509.

LeHuray, A.P., Caulfield, J.B.D., Rye, D.M., and Dixon, P.R., 1987, Basement controls on sediment-hosted Zn-Pb deposits: A Pb isotope study of Carboniferous mineralization in central Ireland: ECONOMIC GEOLOGY, v. 82, p. 1695–1709.

Ludwig, K.R., 1993, ISOPLOT: A plotting and regression program for radiogenic-isotope data (version 2.70): U.S. Geological Survey Open-File Report 91–445 (June 9, 1993 revision), 42 p.

Muller, J.E., 1980, The Paleozoic Sicker Group of Vancouver Island, British Columbia: Canada Geological Survey Paper 79–30, 22 p.

Muller, J.E., Northcote, K.E., and Carlisle, D., 1974, Geology and mineral deposits of the Alert Bay-Cape Scott map-area, Vancouver Island, British Columbia: Canada Geological Survey Paper 74–8, 77 p.

Pearson, C.A., 1993, Mining zinc-rich massive sulphide deposits on Vancouver Island, British Columbia: World Zinc '93 International Symposium, Hobart, Tasmania, Australia, October 1993, Proceedings, p. 75–84.

Robinson, M., 1994, Geology, alteration and mineralization of the Battle zone, Buttle Lake mining camp, central Vancouver Island, southwestern British Columbia: Unpublished M.A.Sc. thesis, Vancouver, University of British Columbia, 268 p.

Robinson, M., and Godwin, C.I., 1995, Genesis of the Blende carbonate-hosted Zn-Pb-Ag deposit, north-central Yukon Territory: Geologic, fluid inclusion and isotopic constraints: ECONOMIC GEOLOGY, v.90, p.369–384.

Robinson, M., Godwin, C.I., and Juras, S., 1994, Major lithologies of the Battle zone, Buttle Lake camp, central Vancouver Island: British Columbia Ministry of Energy, Mines and Petroleum Resources Paper 1994–1, p. 163–177.

Russell, M.J., 1978, Downward-excavating hydrothermal cells and Irish-type ore deposits: Importance of an underlying thick Caledonian prism: Institute of Mining and Metallurgy Transactions, v. 87, section B, p. 168–171.

——1983, Major sediment-hosted exhalative zinc + lead deposits: Formation from hydrothermal convection cells that deepen during crustal extension: Mineralogical Association of Canada Short Course Handbook, v. 9, p. 251–282.

——1986, A model for the genesis of SEDEX deposits [abs.]: Terra Cognita, v. 6, p. 493.

Sada, K., and Danner, W.R., 1974, Early and Middle Pennsylvanian Fusulinids from southern British Columbia, Canada and northwestern Washington, U.S.A.: Palaeontological Society of Japan, Transactions and Proceedings, new series, no. 93, p. 249–265.

Sangster, D.F., 1968, Relative sulphur isotope abundances of ancient seas and stratabound sulphide deposits: Geological Association of Canada Proceedings, v. 17, p. 79–91.

——1972, Precambrian volcanogenic massive sulphide deposits in Canada: A review: Canada Geological Survey Paper 72–22, 44 p.

Sawkins, F.J., and Kowalik, J., 1981, The source of ore metals at Buchans: Magmatic versus leaching models: Geological Association of Canada Special Paper 22, p. 255–268.

Sibson, R.H., Moore, J.M., and Rankin, A.H., 1975, Seismic pumping—a hydrothermal fluid transport mechanism: Geological Society of London Journal, v. 130, p. 101–107.

Smith, A.D., 1993, Geochemistry and tectonic setting of volcanics from the Anyox mining camp, British Columbia: Canadian Journal of Earth Sciences, v. 30, p. 49–59.

Stanton, R.L., 1990, Magmatic evolution and the ore type-lava type affiliations of volcanic exhalative ores: Australasian Institute of Mining and Metallurgy Monograph 14, p. 101–107.

Stanton, R.L., 1991, Understanding volcanic massive sulfides—past, present, and future: ECONOMIC GEOLOGY MONOGRAPH 8, p. 82–95.

Thode, H.G., and Monster, J., 1965, Sulfur isotope geochemistry of petroleum, evaporites and ancient seas: American Association of Petroleum Geologists Memoir 4, p. 367–377.

Walker, R.R., 1985, Westmin Resources' massive sulphide deposits, Vancouver Island: Geological Society of America, Cordilleran Section Meeting, May 1985, Vancouver, B.C., Field Trip Guidebook, p. 1–1 to 1–13.

Whitney, J.A., 1989, Origin and evolution of silicic magmas: Reviews in Economic Geology, v. 4, p. 183–202.

Yole, R.W., 1969, Upper Paleozoic stratigraphy of Vancouver Island, British Columbia: Geological Association of Canada Proceedings, v. 20, p. 30–40.

York, D., 1969, Least-squares fitting of a straight line with correlated errors: Earth and Planetary Science Letters, v. 5, p. 320–324.

Zartman, R.E., and Doe, B.R., 1981, Plumbotectonics—the model: Tectonophysics, v. 75, p. 135–162.